On Ordering of Fundamental Wineglass Modes in Toroidal Ring Gyroscope

Alexandra Efimovskaya, Danmeng Wang, Yu-Wei Lin, and Andrei M. Shkel
MicroSystems Laboratory, University of California, Irvine, CA 92697, USA
Email: {aefimovs, danmenw, yuweil4, ashkel}@uci.edu

***Abstract*—In this paper, we discuss the primary sources of frequency splits in degenerate mode Toroidal Ring Gyroscope (TRG) with isotropic concentric rings suspension. We show that operation in the n=3 "wineglass mode" might be preferable for prioritized device symmetry. We demonstrate that by means of structural design it is possible to achieve a desired order of wineglass modes, critical for vibration immunity, and potentially for improved performance of miniature devices. Mode-ordering is accomplished by a proper choice of a number of rings in the suspension and an angle between the spokes connecting the rings. The method of mode-ordering is confirmed through experimental characterization of 2.8 mm diameter TRG prototypes fabricated in <100> and <111> single crystal silicon.**

***Index Terms*—Coriolis Vibratory Gyroscopes, mode ordering, anisotropy, frequency split.**

I. Introduction

Micromachined degenerate mode Coriolis Vibratory Gyroscopes (CVGs) have recently gained attention due to many favorable features, such as a high rate sensitivity, high signal-to-noise ratio, capability for rate and whole-angle mode operation, and compatibility with advanced self-calibration techniques [1]. However, mechanical elements with a high level of symmetry are required to exploit these advantages.

With the goal of achieving a highly-symmetrical degenerate mode gyroscope, many designs with an isotropic concentric ring suspension emerged in recent years. For example, a 100k Q-factor Toroidal Ring Gyroscope (TRG) with distributed suspension system and outer anchor has been reported in [2]. This device at 1.76 mm diameter was implemented in epitaxial silicon encapsulation process (EpiSeal). Silicon Disk Resonator Gyroscope (DRG) [3] at 8 mm diameter with concentric rings suspension and central support was demonstrated in [4]. A high frequency poly-silicon version of DRG at 0.6 mm diameter was reported in [5].

Axisymmetric structures, such as structures with concentric ring suspension, can possess multiple pairs of nominally degenerate modes in which each pair shows some degree of coriolis coupling (the so-called wine glass modes). Most of the degenerate wineglass mode CVGs are designed to operate in the n=2 or the n=3 wineglass modes. In this paper, we show that the n=3 mode operation might be preferable for prioritized device symmetry. However, the n=2 vibratory mode is usually lower in frequency and is most sensitive to external acceleration, shock, and vibration. We demonstrate that mechanical design allows for reordering the TRG fundamental wineglass modes, placing the n=3 mode before the n=2 mode. Mode-ordering is accomplished by altering a number of rings in the gyroscope suspension and an angle between the spokes. Our study includes a parametric analysis of the gyroscope design and experimental verification.

This material is based upon work supported by DARPA grant N66001-13-1-4021, Program Manager Dr. Robert Lutwak.

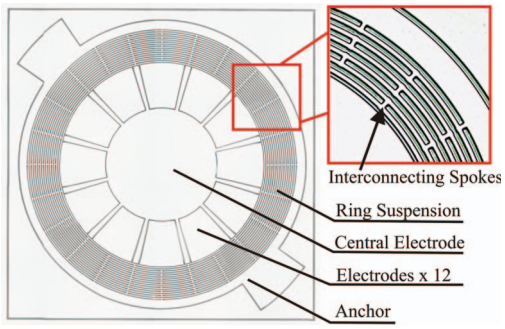

Fig. 1. Microphotograph of a fabricated TRG [2] prototype

II. Toroidal Ring Gyroscope Design

A. Gyroscope Architecture

Toroidal Ring Gyroscope (TRG) is comprised of an inner electrode assembly, an outer support, and a ring suspension, Fig. 1. The TRG is 2.8 mm in diameter, and the suspension system is formed by the 10 μm wide and 100 μm thick concentric rings, each connected by at least four spokes.

The inner electrode assembly consists of radial electrodes that are used as a forcer and as a pick-off, for each of the wineglass modes. The gyroscope, designed to operate in the n=2 mode, includes 8 radial electrodes; the gyroscope, designed to operate in the n=3 mode, includes correspondingly 12 radial electrodes. The central star-shaped electrode has three functions: (1) it acts as a shield by sinking parasitic currents between discrete electrodes, (2) it can function as a DC quadrature null electrode, and (3) it can be used for the gyroscope parametric excitation. Devices are fabricated on single-crystal <100> and <111> Silicon-on-Insulator (SOI) wafers with a 100 μm thick device layer.

B. Fundamental Wineglass Modes

The mechanical element of the gyroscope is a planar resonating structure which has degenerate pairs of in-plane wineglass vibration modes, each of these pairs can be used to measure the Coriolis acceleration induced angular rate signal. TRG can be designed to operate in the n=2 or the

n=3 fundamental modes. Here, n represents a number of pairs of stationary nodes in the vibration pattern, Fig.3. There is typically a trade-off between the implementations. While the n=2 mode operation offers an advantage of a higher angular gain [6], the n=3 mode devices are hypothesized to be inherently more symmetric [2].

There are three primary sources of frequency splits or asymmetry between the two wineglass modes of TRG:

$$\Delta f = \Delta f_1 + \Delta f_2 + \Delta f_3,$$

where Δf_1 is a frequency split due to fabrication imperfections, Δf_2 is induced by misalignment of the mode shapes relative to the orientation of spokes, and Δf_3 is induced by anisotropic modulus of elasticity of crystalline silicon.

The frequency splits Δf_1 due to imperfect fabrication of rings have been studied earlier in [7]. Some fabrication errors that occur in MEMS can be characterized by a few dominant terms in the Fourier expansion of the perturbed geometry. Generally, the effect of geometric imperfections is different for n=2 and n=3 modes, and frequency splitting of each pair of modes depends on the dominant type of perturbations.

The frequency split Δf_2 is induced by the misalignment of the mode shapes relative to the spokes orientation and can be eliminated by using a proper angle of the spokes connecting the concentric rings. For example, in case of the 45° angle between the spokes, the geometric effective stiffness in $\sin(3\theta)$ and $\cos(3\theta)$ directions is the same, Fig. 3(a). Similarly, the geometric effective stiffness in $\sin(2\theta)$ and $\cos(2\theta)$ directions is the same, Fig. 3(b).

For the TRG fabricated on a single-crystal silicon wafer, the material anisotropy has to be considered. It has been shown in literature, that in the case of a single circular ring, the orientation of mode shapes relative to the Si(100) anisotropic elastic modulus curve is the same for the n=3 pair of degenerate modes and different for the n=2 pair of modes [8]. Therefore, the frequency split Δf_3 of an ideal n=3 mode ring is zero and independent of the wafer orientation.

C. Finite Element Analysis

Using Finite Element Analysis (FEA) in ANSYS, we studied the effect of anisotropic elastic constants on the fundamental frequencies of the gyroscope. Table I summarizes the results of modeling of a miniature 2.8 mm diameter TRG. The suspension system is comprised of 16 concentric rings,

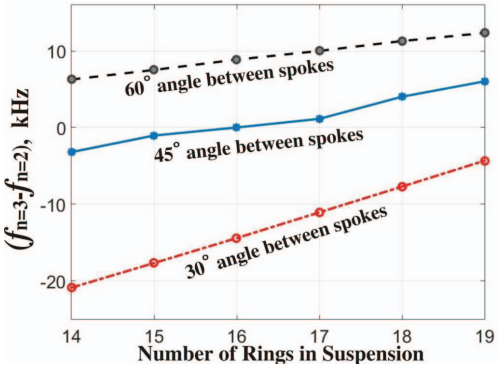

Fig. 2. Separation between n=3 and n=2 pairs of wineglass modes as a function of the number of rings

connected to each other using spokes between the rings at every 45°. The rings are 10 μm wide and 100 μm thick, and the gap between the rings is 10 μm. The modal analysis is performed for a gyroscope implemented in <100> and <111> silicon. Frequency splits of the degenerate modes are estimated for an ideal case and for the case of the wafer plane misaligned from <100> and <111> crystalline planes. In order to simulate the effect of a 1° wafer flat misalignment, we use the corresponding tensor transformation of the single-crystal silicone stiffness matrix [8].

Results of the gyroscope modeling show that for n=3 pair of degenerate modes the frequency split induced by anisotropic modulus of elasticity of crystalline silicon is eliminated and Δf is nearly insensitive to misalignment errors relative to the crystalline orientation of the wafer.

D. Mode-ordering

In case of the large-scale devices, above 5 mm, the high angular-gain factor generally determines the choice of operational modes. In contrast, for the smaller diameter gyroscopes (<3 mm) with a limited electrostatic tuning capability, the symmetry and a small as-fabricated Δf have to be often prioritized. For the smaller diameter TRG, the n=3 mode of operation is preferable.

However, the n=2 vibratory mode of the degenerate wineglass mode gyroscope is usually lower in frequency and is most sensitive to external acceleration. Therefore, it is necessary to order the modes, placing the n=3 mode at lower frequency than the n=2 mode.

TABLE I
FINITE ELEMENT ANALYSIS (FEA) OF THE TRG NATURAL FREQUENCIES

		n=2		n=3	
Si(1-0-0)	**Ideal**	*fc=28.25 kHz*	Δf *=839 Hz*	*fc=28.68 kHz*	Δf *=0 Hz*
	1°off in [001]-direction	*fc=28.25 kHz*	Δf *=838.6 Hz*	*fc=28.68 kHz*	Δf *=0.4 Hz*
	1°off in [010]-direction	*fc=28.25 kHz*	Δf *=838.6 Hz*	*fc=28.68 kHz*	Δf *=0.4 Hz*
	1°off in [100]-direction	*fc=28.25 kHz*	Δf *=839.5 Hz*	*fc=28.68 kHz*	Δf *=0 Hz*
Si(1-1-1)	**Ideal**	*fc=29.97 kHz*	Δf *=0 Hz*	*fc=30.64 kHz*	Δf *=0 Hz*
	1°off in [01-1]-direction	*fc=29.97 kHz*	Δf *=18.2 Hz*	*fc=30.63 kHz*	Δf *=0.1 Hz*
	1°off in [2-1-1]-direction	*fc=29.97 kHz*	Δf *=21.7 Hz*	*fc=30.59 kHz*	Δf *=0.2 Hz*
	1°off in [111]-direction	*fc=29.97 kHz*	Δf *=0 Hz*	*fc=30.64 kHz*	Δf *=0 Hz*

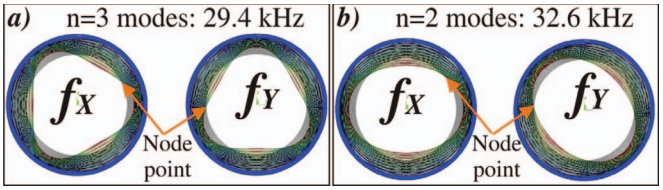

Fig. 3. TRG was designed to operate at the resonant freq. of 29.4 kHz in the n=3 mode, which has the lowest stiffness among all wineglass modes.

Using FEA, we explored the frequency separation between the n=2 and n=3 pairs of wineglass modes as a function of the number of rings and the angle between the interconnecting spokes. Fig. 2 shows that the split between two pairs of degenerate modes decreases with reduction in the number of concentric rings in the suspension; the n=2 and the n=3 wineglass modes eventually switch the order. For example, for the design with 14 rings and a 45° angle between the spokes, it is possible to place the n=3 modes before the n=2 modes and achieve a 3.2 kHz frequency separation between two pairs of degenerate modes, Fig.3.

III. Experimental Results

Prototypes of a miniature 2.8 mm diameter TRG with 45° and 30° angle between the spokes are fabricated in <100> and <111> silicon wafers with a 100 μm thick device layer, Table II. Frequency response of the gyroscopes is tested using electrostatic actuation and capacitive detection. Experimental characterization shows that the mode-ordering is achieved for all fabricated prototypes: the n=3 modes are the lowest in frequency among all the wineglass modes. The frequency separation between the two pairs of the degenerate modes is in the range from 2.6 to 19.6 kHz.

The TRG with 14 rings and 45° angle between the spokes, implemented in <111> silicon, is excited using the DC bias voltage of 18V DC and the AC voltage of 0.8V, applied to the n=3 mode radial electrodes. We observed two high in amplitude resonant peaks at 25.47 kHz with Δf of 10 Hz, corresponding to the n=3 wineglass modes and two lower in amplitude peaks at 28.13 kHz with Δf of 36 Hz, corresponding to the n=2 modes. The separation between the two pairs of degenerate modes is 2.6 kHz, Fig.4. This result shows a good match between the experiment and the FEA.

Gyroscope samples 1-5 in Table II exhibit a significantly higher frequency split of the n=2 modes. In case of 30° angle between the spokes, high Δf is attributed to misalignment of the n=2 mode shapes relative to the spokes orientation, resulting in difference in effective stiffness of the two modes.

IV. Conclusion

In this work, we reviewed the main sources of frequency splits in degenerate mode Toroidal Ring Gyroscope (TRG) with concentric rings suspension. The trade-offs of operation in the n=2 and the n=3 wineglass modes have been discussed. While the n=2 mode offers an advantage of a higher angular gain factor, the n=3 mode devices are inherently more symmetric, resulting in a lower as-fabricated frequency split Δf.

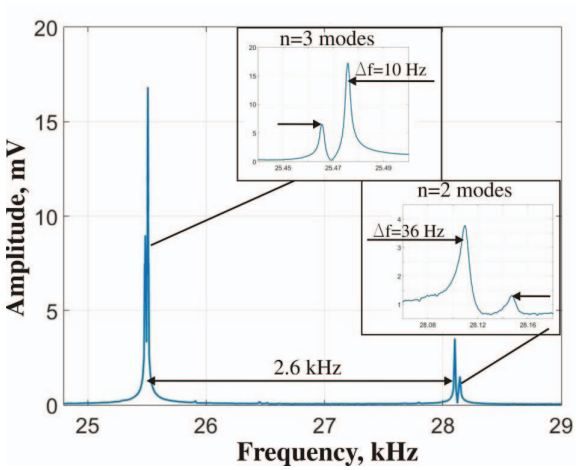

Fig. 4. Experimental freq. response of the TRG with 14 rings and a 45° angle between the spokes, showing successful mode ordering.

TABLE II
Experimental Frequency Response Characterization of TRG

	No	Spokes Angle	n=2		n=3	
			fc, kHz	$\Delta f, Hz$	fc, kHz	$\Delta f, Hz$
Si (1-0-0)	1	30	49.5	3500	35.10	50
	2	30	50.56	3720	32.33	26
Si (1-1-1)	3	30	53.74	1603	34.18	4
	4	30	52.6	1587	34.55	15
	5	30	51.47	1500	32.5	14
	6	45	28.13	36	25.47	10

We demonstrated a possibility to achieve the desired mode-ordering by a proper choice of the number of rings in the gyroscope suspension and the angle between the spokes connecting the rings. Our method of fundamental wineglass modes ordering was validated through the experimental characterization of the TRG prototypes.

Acknowledgment

This material is based upon work supported by DARPA grant N66001-13-1-4021. Devices were designed, developed, and tested in MicroSystems Laboratory, UC Irvine.

References

[1] A. Trusov, et al., *Force Rebalance, Whole Angle, and Self-Calibration Mechanization of Silicon MEMS Quad Mass Gyro*, IEEE ISISS 2014, Laguna Beach, CA, USA, February 25-26, (2014).
[2] D. Senkal, et al., *100k Q-Factor Toroidal Ring Gyroscope Implemented in Wafer-level Epitaxial Silicon Encapsulation Process*, IEEE MEMS 2014, San Francisco, CA, USA, January 26-30, (2014).
[3] R.L. Kubena, et al., *Disc Resonator Gyroscopes*, US Patent 7,581,443, (2009).
[4] A. D. Challoner, et al., *Boeing Disc Resonator Gyroscope*, Proc. IEEE/ION Position, Location and Navigation Symposium - PLANS 2014, Monterey, USA, May 5-8, (2014).
[5] S. Nitzan, et al., *Epitaxially-encapsulated polysilicon disk resonator gyroscope*, IEEE MEMS, pp. 625-628, (2013).
[6] D. D. Lynch, *Coriolis Vibratory Gyros*, Proc. Symposium Gyro Technology, Stuttgart, Germany, (1998).
[7] E. Yilmaz, et al., *Effects of Imperfections on Solid-Wave Gyroscope Dynamics*, Proc. IEEE SENSORS, Baltimore, USA, Nov. 3-6, (2013).
[8] C. O. Chang, et al., *In-plane free vibration of a single-crystal silicon ring*, Journal of Solids and Structures, vol. 45, pp. 61146132, (2008).